

EFFECT OF MOLECULAR WEIGHT AND DEGREE OF ACETYLATION ON THE PHYSICOCHEMICAL CHARACTERISTICS OF CHITOSAN NANOPARTICLES

Goycoolea F.M.^{1,2}, El Gueddari N. E.³, Remuñán-López C.¹, Coggiola A.¹, Lollo G.¹, Domard A.⁴ and Alonso M.J.^{1*}

¹*Universidad de Santiago de Compostela. Facultad de Farmacia. Departamento de Farmacia y Tecnología Farmacéutica. Campus Sur s/n. 15782 Santiago de Compostela, A Coruña, Spain*

²*Laboratory of Biopolymers. CIAD. P.O.Box 1735, Hermosillo, Sonora, 83000, Mexico*

³*IBBP, University of Münster, 48143, Münster, Germany*

⁴*Laboratoire des Matériaux Polymères et des Biomatériaux – UMR CNRS 5627, Domaine scientifique de la Doua, Bâtiment ISTIL, 15, Bd A. Latarjet, 69622, Villeurbanne Cedex France*

*E-mail address: ffmjalon@usc.es

INTRODUCTION

Chitosan (CS)-based nanoparticles have been a focus of increasing attention in recent years, particularly for the design and engineering of novel nanoparticulate drug delivery systems, due to their desirable properties such as biocompatibility, biodegradability, bio- and mucoadhesivity, and hydrophilic character that facilitate the administration of poorly absorbable drugs across various epithelial barriers, such as corneal, nasal and intestinal mucosa [1]. An additional advantage of this type of system is that they can be produced under aqueous and fairly mild conditions, thus effectively, being especially suitable to preserve the bioactive conformation of delicate macromolecules (e.g. hormones, antigens, DNA, siRNA, growth factors), that otherwise would be prone to enzymatic degradation and hydrolysis [2,3]. Most frequently chitosan nanoparticles are formed according to a bottom-up approach as a result of a self-assembling or crosslinking processes in which the molecules arrange themselves into ordered nanoscale structures either by physical or covalent inter- or intramolecular interactions. In these nanostructures, the drug can be entrapped or attached to the nanoparticle matrix. CS nanoparticles have been prepared by several methodologies, including physical crosslinking by ionic gelation by specific ions such as pentasodium tripolyphosphate (TPP) [4] or EDTA [5]. In particular, CS-TPP nanoparticles have been utilized as a drug delivery platform for a wide range of active molecules [1]. A recognized feature of these nanosystems is their capacity to protect hydrophilic macromolecules against degradation and their ability to overcome mucosal barriers. As a consequence, their application has been mainly centred in non invasive routes of administration via ocular, nasal and oral and oral mucosae [2,6-9].

From the physicochemical standpoint the interaction of CS with TPP is accepted to be mediated by the intramolecular crosslinking of tripolyphosphoric ($P_3O_5^{5-}$ and $HP_3O_4^{4-}$) ionic species, product of the dissociation of TPP in aqueous solution, with $-NH_3^+$ groups in CS. The effect of pH, ionic strength and other preparative conditions and intrinsic characteristics of CS on the physical characteristics of CS-TPP nanoparticles has been studied, with attention to the ratio of CS to TPP [10-13], as well as to the M_w [14,15] and DA [12] of CS. Several features can generally be recognized in CS-TPP nanoparticles

obtained under various preparation conditions using CS samples of different M_w and DA: an average diameter varying in the range ~ 100 to ~ 350 nm; a surface positive zeta potential (ζ); and a spherical morphology as visualized under transmission electron microscopy (TEM). This study aimed to assess systematically and deepen the understanding of the effect of the intrinsic characteristics of CS on the physical and stability properties of CS nanoparticles crosslinked with TPP, with attention to the role of the weight-average molecular weight (M_w) and degree of acetylation (DA) of CS with a series of samples obtained from a single CS batch.

MATERIALS and METHODS

Materials. The parent CS sample was supplied by Dr. Dominique Gillet of Mahtani Chitosan Pvt Ltd (France). The supplier characteristics for this CS sample were: $M_w \sim 435$ kDa, DA 1.6% (Ref No. 113 batch No 17/12/04). All reagents were of analytical grade and Milli-Q water was used throughout.

Purification, depolymerization and N-acetylation of CS. The parent CS was dissolved in 5% stoichiometric excess of acetic acid and filtered successively through 3, 0.8, and 0.45 μm pore size membranes (Millipore). Purified CS was subsequently depolymerized under nitrous acid generated from NaNO_2 [16] in order to obtain two sample batches of high degree of polymerization ($M_w \sim 120$ kDa) and low degree of polymerization ($M_w \sim 10$ kDa). A portion of both CS samples was N-acetylated under homogeneous conditions by adding the needed stoichiometric amount of acetic anhydride in 1,2-propanediol so as to afford CS samples with DA varying in the range 1.4 to 56% [17].

Characterization of CS. The molecular weight distribution of the CS samples was determined by SEC-HPLC coupled with MALLS and DRI multidetection [18]. The specific refractive index dn/dc values used were those estimated independently by interferometry (NFT ScanRef) and known to vary with the of DA of CS [19]. The degree of acetylation on CS samples was determined by ^1H NMR spectroscopy. To this end, CS samples were dissolved in dilute acidic D_2O (at pD 3–4) as proposed elsewhere [20]. Spectra were recorded on a Bükker-Spectrospin AM 300 spectrometer (300 MHz). Approximately 200–250 scans were acquired.

Preparation and characterization of CS-TPP nanoparticles. Nanoparticles were spontaneously formed by the rapid mixing of 1.0 mL of a TPP solution into 3 mL of the CS solution in acetic acid in a test tube under magnetic stirring (~ 200 rpm) at room temperature [4]. Agitation was maintained for 10 min to allow complete stabilization of the nanosystem. The nanoparticles were isolated by centrifugation ($10000 \times g$, 40 min, 25°C) in tared eppendorff vials containing ~ 20 μL of glycerol previously placed at the bottom of the vial. The CS:TPP mass ratio was fixed at 4:1. The size of nanoparticles was determined by non-invasive back scattering (NIBS) and the value of ζ by by mixed laser Doppler velocimetry and phase analysis light scattering (M3-PALS) using a Malvern Zetasizer NanoZS (Malvern Instruments UK). The ultrastructure of the nanoparticles was investigated by transmission electron microscopy TEM on a Philips CM12 instrument (Eindhoven, The Netherlands).

Stability studies. The colloidal stability of the nanoparticles in HBSS buffer (pH ~ 6.2) was evaluated in terms of the evolution of the particle size with time during incubation at 25 and 37°C . Size measurements at given time intervals were registered as described above.

RESULTS and DISCUSSION

A total of eight sample batches of purified CS of high (~120-260 kDa, HDP) and low (~11–13 kDa, LDP) degree of polymerization and DA values varying in the range 1.6 to 56% were obtained. The characteristics of these CS are summarized in Table 1. It is worth

Table 1. Physicochemical characteristics of chitosan samples

High degree of polymerization (HDP)				
DA(%) ^a	1.6	11.0	27.5	56.0
M_w ^b	123900	122100	143000	266100
M_n ^b	89000	75330	85710	139700
I_p ^b	1.39	1.62	1.67	1.90
R_z (nm) ^b	59.7	45.8	53.8	96.3
DP ^c	766	737	818	1442
Low degree of polymerization (LDP)				
DA(%) ^a	1.4	9.2	27.8	51
M_w ^b	13200	9572	11530	11420
M_n ^b	11130	5914	8120	6012
I_p ^b	1.19	1.62	1.42	1.90
R_z (nm) ^b	82.1	59.6	30.4	37.1
DP ^c	82	58	67	63

^a Degree of acetylation as determined by ¹H NMR.

^b Parameters determined by GPC–HPLC with multidetection (MALLS–DRI): weight average molecular weight (M_w); number average molecular weight (M_n); polydispersity index ($I_p = M_w/M_n$); and radius of gyration (R_z).

^c Degree of polymerization ($DP = M_w / \text{molar mass per residue}$).

to mention that the observed apparent increase in M_w of HDP samples with DA can be attributed to a self-aggregation effect and perhaps do not reflect the real M_w of individual polymer chains. This effect is not observed in LDP CS samples.

The eight CS samples described above of varying M_w and DA were used to prepare nanoparticles by ionotropic crosslinking with TPP. In general, LDP CS allowed to obtain nanoparticles under a yield varying in the range ~30–40%, while for nanoparticles from HDP CS the upper range went up to ~80%. Figure 1 shows the variation of particle size with the degree of acetylation for the full series of samples. Inspection of Fig. 1a reveals that the particle size showed a moderate increase with the degree of acetylation for nanoparticles prepared from LDP chitosan. While for nanoparticles harnessed from HDP this increase was more pronounced particularly for samples with DA > 27%. In turn, ζ values decreased with DA under a rather uniform dependence for LDP CS from ~+35 to ~+27 mV, while nanoparticles obtained from HDP CS exhibited a slight increment (~+32 to ~+37 mV) in ζ as DA increased from 1.6 to 27.5 %, and a drastic drop in ζ when the DA increased to 56%. These results are consistent with the idea that the presence of N–acetyl groups in CS leads to the creation of more expanded structures, perhaps due to the formation of ‘loops’ formed by local zones where TPP does not form cooperative crosslinking bridges between $-\text{NH}_3^+$ groups in D–glucosamine residues. The formation of these type of structures has been proposed to explain the effect of the pH over the degree of protonation of $-\text{NH}_3^+$ groups in CS–TPP gel beads [21].

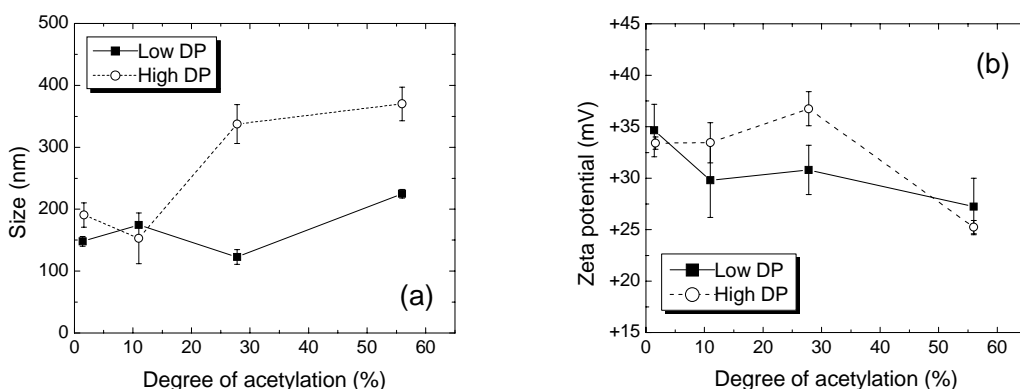


Figure 1. Variation of a) size and b) zeta potential of chitosan-pentasodium tripolyphosphate (CS-TPP) nanoparticles with the degree of acetylation of chitosan of low ($M_w \sim 10$ kDa) and high ($M_w \sim 120$ kDa) degree of polymerization (as indicated in legend; CS:TPP mass ratio was fixed to 4:1 in all cases). Data represent mean average of triplicate analysis (\pm standard error).

The tendency to form ‘loops’ would be expected to be more favoured in larger CS chains than in shorter ones that can be conceived as more densely packed into gelled nanoparticles (Fig. 1a). In turn, the consequence of the formation of these ‘loops’ in HDP CS nanoparticles may lead to the creation of zones of greater local hydrophobicity, that would preferably be oriented towards the inner side of the nanoparticle matrix. This agrees well with the marginal increment observed in ζ with DA up to DA 27% (Fig. 1b). The dramatic decrease in ζ of nanoparticles of HDP CS of DA 56% may reflect that a different structural rearrangement takes place in these nanoparticles as they are unable to accommodate all the hydrophobic neutral groups inwards. While for LDP CS-based nanoparticles, the more regular decrease in zeta potential may be only a consequence of the lower proportion of net charged $-\text{NH}_3^+$ groups in the system that are evenly distributed in the surface and inner matrix of the nanoparticle. The morphology of the nanoparticles was invariably spherical as evidenced by TEM micrographs (Fig. 2). From the micrographs, it can be appreciated that nanoparticles obtained from LDP CS (Fig. 2a) appear as more dense and compact than those obtained from HDP CS at equivalent DA (Fig. 2b). In turn, nanoparticles of HDP CS of high DA (Fig. 2c), appear as larger structures in general accordance with results and interpretations from NIBS measurements shown in Fig. 1a.

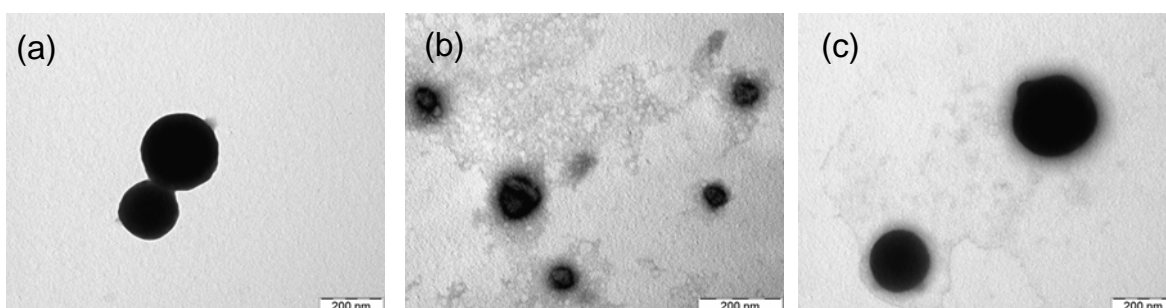


Figure 2. TEM micrographs of chitosan-TPP nanoparticles prepared from chitosan samples of varying M_w and DA as: a) LDP DA 9.2%; b) HDP DA 11% and c) HDP DA 56%.

The stability of CS–TPP nanoparticles in HBSS buffer of pH 6.2 was crucial so as to anticipate the potential use of this nanoparticle system in cell culture studies. Figure 3 shows the variation of the size of CS–TPP nanoparticles prepared from HDP CS in this buffer system at 25 and at 37°C. Notice in Figure 2a that in general, at 25°C the system was stable up to 30 min, with virtually no change in particle size irrespectively of the degree of acetylation. However, at 37°C (Fig. 3b) the nanoparticles of DA ~56% grew into large aggregates over a period of 30 min. Interestingly, the nanoparticles from CS of DA ~1.6% were completely unstable at 37°C and it was impossible to register their size. The lower stability of the CS–TPP nanoparticles made out of HDP CS of DA 56% observed at 37°C and not at 25°C, can be explained in terms of hydrophobic–driven aggregation of N–acetyl groups at the surface of the nanoparticle, as explained above, and it is consistent with the observed reduction in zeta potential for these nanoparticles (Fig. 1b). We do not fully understand as yet why the nanoparticles comprising CS of lowest DA were also unstable at 37°C, however, this may be due to the sensitivity of this system in a medium of a high concentration of electrolytes [13]. Essentially similar results were found for the nanoparticles prepared from LDP CS (results not shown). However, in this case, at 37°C only the nanoparticles of DA ~ 1.4 were found to be stable in HBSS buffer.

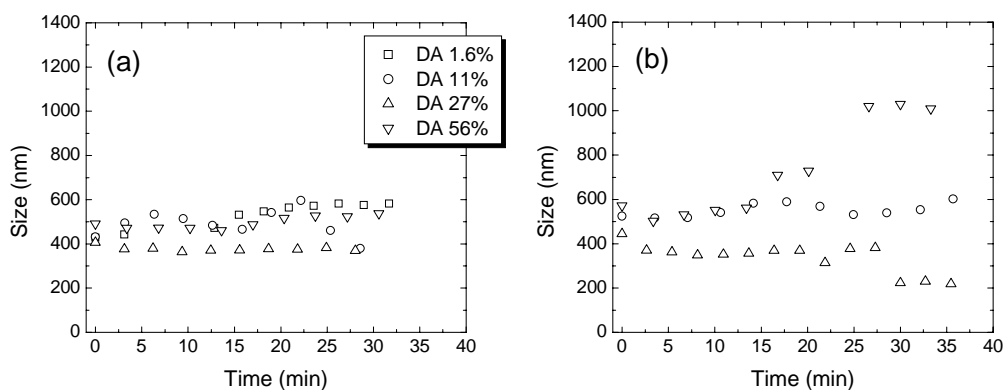


Figure 3. Evolution of the diameter size with time of HDP ($M_w \sim 120$ kDa) chitosan–TPP nanoparticles made of chitosan of varying degree of acetylation (as indicated in legend) re-suspended in HBSS buffer of pH ~6.2 (CS:TPP mass ratio was fixed to 4:1 in all cases) at (a) 25 and (b) 37°C.

The experimental evidence of this study is consistent with the proposal that at high DA the properties of CS–TPP nanoparticles are governed by the hydrophobicity conferred by N–acetylated residues located at the surface. In a next stage the bioactive properties of the different nanoparticles systems will be addressed.

ACKNOWLEDGEMENTS

Financial support of the European Union from the NANOBIOCHARIDES project (Ref No. 013882 of call FP6–2003–NMP–TI–3–Main) is gratefully acknowledged.

REFERENCES

- [1] Alonso, M. J., Prego, C., and García–Fuentes, M. (2007) Polysaccharide–based nanoparticles as carriers for drug and vaccine delivery. In *Nanoparticles for Pharmaceutical Application* (Domb, J.; Tabata, Y.; Ravi Kumar, M. N. V. and Farber, S. eds.), pp. 135–50, American Scientific Publishers.
- [2] Csaba, N., García–Fuentes, M., and Alonso, M. J. (2006) The performance of nanocarriers for transmucosal drug delivery. *Expert. Opin. Drug Deliv.*, 3, 463–78

- [3] Janes, K. A., Calvo, P. and Alonso, M. J. (2001) Polysaccharide colloidal particles as delivery systems for macromolecules. *Adv. Drug Del. Rev.*, 47, 83–97.
- [4] Calvo, P., Remuñán-López, C., Vila-Jato, J. L., and Alonso, M.J. (1997) Novel hydrophilic chitosan–polyethylene oxide nanoparticles as protein carriers. *J. Appl. Polym. Sci.*, 63 125–32.
- [5] Loretz, B. and Bernkop-Schnürch, A. (2006) In vitro evaluation of chitosan–EDTA conjugate polyplexes as a nanoparticulate gene delivery system. *AAPS J.* 8 (4), art. no. 85
- [6] Sanchez, A. and Alonso, M. J. (2006) Nanoparticulate carriers for ocular drug delivery. In *Nanoparticles as Drug Carriers* (Torchilin, V. ed.), pp. 649–74, World Scientific–Imperial College Press.
- [7] Alonso, M. J. and Sanchez, A. (2003) The potential of chitosan in ocular drug delivery. *J. Pharm. Pharmacol.*, 55, 1451–63.
- [8] Prego, C., Torres, D. and Alonso, M. J. (2005) The potential of chitosan for the oral administration of peptides. *Expert. Opin. Drug Del.*, 2, 843–54.
- [9] Goycoolea, F. M., Higuera-Ciajara, I. and Alonso, M. J. (2007) Polysaccharide nanoparticles based on chitosan: a growing class of nanomaterials for biopharmaceutical applications. In *Handbook of Natural-based Polymers for Biomedical Applications* (Reis, R. ed.). Woodhead Publishing Ltd. In Press
- [10] Gan, Q., Wang, T., Cochrane, C. and McCarron, P. (2005) Modulation of surface charge, particle size and morphological properties of chitosan–TPP nanoparticles intended for gene delivery. *Colloid Surface B*, 44, 65–73.
- [11] Zhang, H., Oh, M., Allen, C. and Kumacheva, E. (2004) Monodisperse chitosan nanoparticles for mucosal drug delivery. *Biomacromolecules*, 5, 2461–68.
- [12] Xu, Y. and Du, Y. (2003). Effect of molecular structure of chitosan on protein delivery properties of chitosan nanoparticles, *Int. J. Pharm.*, 250, 215–26.
- [13] López-León, T., Carvalho, E. L. S., Seijo, B., Ortega-Vinuesa, J. L. and Bastos-González, D. (2005) Physicochemical characterization of chitosan nanoparticles: electrokinetic and stability behaviour. *J. Colloid Interf. Sci.*, 283, 344–51.
- [14] Janes, K. A. and Alonso, M. J. (2003) Depolymerized chitosan nanoparticles for protein delivery: preparation and characterization. *J. Appl. Polym. Sci.*, 88, 2769–76.
- [15] Vila, A., Sánchez, A., Janes, K. A., Behrens, I., Kissel, T., Vila-Jato, J. L. and Alonso, M. J. (2004) Low molecular weight chitosan nanoparticles as new carriers for nasal vaccine delivery in mice. *Eur. J. Pharm. Biopharm.*, 57, 123–31
- [16] Allan, G. G. and Peyron, M. (1995) Molecular weight manipulation of chitosan I: Kinetics of depolymerization by nitrous acid. *Carbohydr. Res.* 277, 257–72
- [17] Lamarque, G.; Lucas, J.L.; Viton C. and Domard A. (2005) Physicochemical behavior of homogeneous series of acetylated chitosans in aqueous solution: Role of various structural parameters. *Biomacromolecules*, 6, 131–42
- [18] Sorlier, P., Viton C. and Domard, A. (2002). Relation between solution properties and degree of acetylation of chitosan: Role of aging. *Biomacromolecules*, 3, 1336–42.
- [19] Schatz, C., Pichot, C., Delair, T., Viton, C., and Domard, A. (2003). Static light scattering studies on chitosan solutions: From macromolecular chains to colloidal dispersions. *Langmuir*, 19, 9896–903
- [20] Hirai, A., Odani, H. and Nakajima, A. (1991). Determination of degree of deacetylation of chitosan by ¹H NMR spectroscopy. *Polymer Bull*, 26, 87–94.
- [21] Mi, F. L., Shyu, S. S., Wong, T. B., Jang, S. F., Lee, S. T. and Lu, K. T. (1999) Chitosan–polyelectrolyte complexation for the preparation of gel beads and controlled release of anticancer drug. II. effect of pH–dependent ionic crosslinking or interpolymer complex using tripolyphosphate or polyphosphate as reagent. *J. Appl. Polym. Sci.*, 74, 1093–107.